



Phase separated behavior in yttrium doped CaMnO_3



Neetika Sharma^a, A. Das^{a,*}, C.L. Prajapat^b, Amit Kumar^a, M.R. Singh^b

^a Solid State Physics Division, Bhabha Atomic Research Centre, Trombay, Mumbai 400085, India

^b Technical Physics Division, Bhabha Atomic Research Centre, Trombay, Mumbai 400085, India

ARTICLE INFO

Article history:

Received 24 August 2015

Received in revised form 1 February 2016

Accepted 6 February 2016

Available online 9 February 2016

Keywords:

- A. Magnetic materials
- B. Chemical synthesis
- C. Neutron diffraction
- D. Magnetic properties
- E. Magnetic structure

ABSTRACT

The effect of electron doping on the structural, transport, and magnetic properties of Mn (IV)—rich $\text{Ca}_{1-x}\text{Y}_x\text{MnO}_3$ ($x \leq 0.2$) samples have been investigated using neutron diffraction, neutron depolarization, magnetization and resistivity techniques. The temperature dependence of resistivity follows the small polaron model and the activation energy exhibits a minimum for $x=0.1$ sample. A phase separated magnetic ground state consisting of ferromagnetic domains ($\sim 7 \mu\text{m}$) embedded in G-type antiferromagnetic matrix is observed in the sample, $x=0.1$. The transition to the long-range magnetically ordered state in this sample is preceded by a Griffith's phase. On lowering temperature below 300 K a structural transition from orthorhombic structure ($Pnma$) to a monoclinic structure ($P2_1/m$) is observed in the case of $x=0.2$ sample. The ferromagnetic behavior in this case is suppressed and the antiferromagnetic ordering is described by coexisting C-type and G-type magnetic structures corresponding to the monoclinic and orthorhombic phases, respectively.

© 2016 Elsevier Ltd. All rights reserved.

1. Introduction

The hole doped manganites $\text{A}_x\text{A}_{1-x}\text{MnO}_3$ exhibit several interesting behavior viz., colossal magnetoresistance (CMR), charge, spin and orbital coupling, and mesoscopic phase separation. A strong correlation between the charge, spin, and orbital degrees of freedom in these compounds makes them sensitive to external perturbations, such as temperature, magnetic field, external pressure, and average A-site ionic radii [1,2]. The physical properties of these compounds are mostly governed by Zener double-exchange mechanism of electron hopping, superexchange interactions, and Jahn-Teller type electron-phonon interactions [3]. The effect of hole doping in the manganites has been studied in great detail but only a few studies are available on the effect of electron doping on their magnetic properties.

The varied magnetic structures observed in the series $\text{La}_{1-x}\text{Ca}_x\text{MnO}_3$ system have been described by Wollan and Koehler [4]. CaMnO_3 crystallizes in the perovskite related GdFeO_3 -type orthorhombic structure and exhibits a G-type antiferromagnetic (AFM) structure ($T_N \sim 125 \text{ K}$) with a weak ferromagnetic component in its ground state [5]. In this structure each Mn moment is coupled antiferromagnetically with its nearest Mn neighbors. However, doping with trivalent ions at Ca^{2+} site is found to give rise to ferromagnetic (FM) behavior in these compounds. The role of

spin canting and/or phase separation leading to FM behavior in these compounds has been a subject of debate in the literature. The ferromagnetic behavior in the series of compounds $\text{Ca}_{1-x}\text{La}_x\text{MnO}_3$ has been shown to be intrinsic in origin and is found to couple strongly with the lattice leading to a complex structural and magnetic phase diagram [6,7]. The transport and magnetic properties of some of the electron doped manganites $\text{Ca}_{1-x}\text{A}_x\text{MnO}_3$ ($\text{A} = \text{Pr, Nd, Eu, Gd, Ho, Sm, Ce, Th}$) are found to be governed by the electron concentration [8,9] as against the dominating influence of average A-site ionic radii observed in the case of hole doped manganites. Phase separation behavior has been reported for Sm [9] and Pr [10] doped CaMnO_3 whereas the magnetic ground for the Ho [11] doped compound is identified as a spin canted antiferromagnet. Similar studies on Ru doped CaMnO_3 show phase separated FM + AFM ground state [12]. However, the antiferromagnetic structure of Mo doped CaMnO_3 was found to be A_xFyG_z type and a clear distinction between phase separation and spin canting behavior in this compound could not be established [13].

These studies therefore, show that the nature of magnetic ordering in electron doped manganites is varied and inconclusive. Doping CaMnO_3 with Y^{3+} ion which is non magnetic and similar to La^{3+} , albeit with lower ionic radii, it was expected, that an equally complex magnetic phase diagram would emerge [14,15]. However, a previous study on Y doped CaMnO_3 could not establish the presence of either phase-separation or homogeneous canted AFM magnetic structure [14]. We have investigated the isostructural $\text{Ca}_{1-x}\text{Y}_x\text{MnO}_3$ ($0 \leq x \leq 0.2$) compounds and show that a phase

* Corresponding author.

E-mail address: adas@barc.gov.in (A. Das).

separated behavior, with coexisting short range ferro- and long range antiferromagnetic ordering describes the magnetic state of $x=0.1$ compound. At higher doping ($x=0.2$), the orthorhombic phase partially transforms to a monoclinic phase. Antiferromagnetic ordering of type G_z for the orthorhombic structure and C-type ordering for the monoclinic structure is observed in this case. Our experimental results are not in agreement with the recently concluded spin canting behavior observed theoretically [16] and experimentally in Ce-doped CaMnO_3 [17].

2. Experimental details

Polycrystalline samples of $\text{Ca}_{1-x}\text{Y}_x\text{MnO}_3$ ($x=0.1, 0.2$) were synthesized using conventional solid-state reaction methods. The starting material CaCO_3 , MnO_2 and Y_2O_3 were mixed in stoichiometric ratios and heated in air at 1100°C for 30 h, 1150°C for 20 h, and 1300°C for 30 h, successively with intermediate grindings. X-ray powder diffraction patterns were recorded using $\text{Cu K}\alpha$ radiation in the angular range $10^\circ \leq 2\theta \leq 70^\circ$ on a Rigaku make diffractometer. The dc resistivity measurements were carried out using standard four probe technique. The magnetization measurements were recorded on a SQUID magnetometer (Quantum Design). Neutron depolarization measurements ($\lambda = 1.205 \text{ \AA}$) were carried out on the polarized neutron spectrometer at Dhruva reactor, Bhabha Atomic Research Centre, Mumbai, India, with Cu_2MnAl (111) as polarizer and $\text{Co}_{0.92}\text{Fe}_{0.08}$ (200) as analyzer. Neutron diffraction patterns were recorded on the PD2 powder diffractometer ($\lambda = 1.2443 \text{ \AA}$) at the Dhruva reactor, Bhabha Atomic Research Centre, Mumbai in the angular range $5^\circ \leq 2\theta \leq 140^\circ$. The Rietveld refinement of the neutron diffraction patterns were carried out using FULLPROF program [18].

3. Results and discussion

The Rietveld refinement of the room temperature x-ray diffraction pattern confirms the single-phase nature of the studied samples $\text{Ca}_{1-x}\text{Y}_x\text{MnO}_3$ ($0 \leq x \leq 0.2$) and is shown in Fig. 1. All the samples crystallize in the orthorhombic phase (space group $Pnma$) at 300 K. The cell parameters of $\text{Ca}_{0.9}\text{Y}_{0.1}\text{MnO}_3$ sample follow the relation $a > b/\sqrt{2} > c$ in the temperature range $6\text{K} \leq T \leq 300\text{K}$,

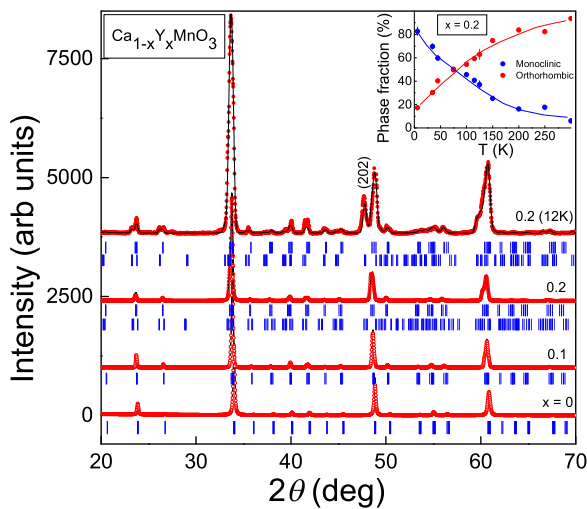


Fig. 1. X-ray diffraction patterns of $\text{Ca}_{1-x}\text{Y}_x\text{MnO}_3$ ($0 \leq x \leq 0.2$) at 300 K and $x=0.2$ at 12 K. Open circles are observed data points. The solid line represents the Rietveld refinement. The tick marks indicate the position of nuclear Bragg peaks. In the case of $x=0.2$ sample the upper and lower tick marks indicate the position of reflections in Orthorhombic and monoclinic phase, respectively. The plots for $x=0.1$ and 0.2 are offset vertically for clarity. Inset shows the temperature variation of the monoclinic and orthorhombic phase fraction for $x=0.2$. The solid lines are the guide to the eye.

which corresponds to an O-type orthorhombic structure. This structure results from a cooperative buckling of the corner shared octahedra [19]. No evidence of monoclinic phase is found in this compound on lowering of temperature. Therefore, we have analyzed the neutron diffraction data of $x=0.1$ sample in the $Pnma$ space group alone. However, analysis of the x-ray and neutron diffraction data at 12 K for $\text{Ca}_{0.8}\text{Y}_{0.2}\text{MnO}_3$ sample shows that this sample exhibits a monoclinic phase ($P2_1/m$ space group) in addition to the orthorhombic phase. Clear distinct reflections arising from the monoclinic phase are observed in the x-ray diffraction pattern recorded at 12 K for $x=0.2$ (Fig. 1). Therefore, a two phase refinement, including both orthorhombic and monoclinic phases has been carried out for this sample. At 6 K the monoclinic phase is found to be dominant with 82% volume fraction. The fraction of monoclinic phase gradually decreases with increase in temperature and at 300 K the fraction of monoclinic phase is very small ($\sim 6\%$), as shown in the inset of Fig. 1. In this sample, the orthorhombic cell parameters exhibits $a > b/\sqrt{2} > c$ at 300 K. The unit cell volume, increases with Y substitution despite the lower ionic radius of Y^{3+} (1.07 \AA) as compared to Ca^{2+} (1.18 \AA). The observed increase in volume, therefore, results from the larger ionic radius of Mn^{3+} (0.645 \AA) as compared to Mn^{4+} (0.530 \AA) in six coordinated state which compensates for the difference of ionic radii between Ca^{2+} and Y^{3+} ions [20]. The difference in ionic radii of Ca^{2+} and Y^{3+} leads to ionic-size disorder which is quantified by the A-cation radius distribution expressed as $\sigma^2 = \sum x_i r_i^2 - \langle r \rangle^2$, where x_i is the fractional occupancy of the A-site ion, r_i is the corresponding ionic radius and $\langle r \rangle$ is the average A-site ionic radius [21,22]. The $\langle r \rangle$ decreases with increase of the Y^{3+} content because of the lower ionic size of Y ion. This reduction in $\langle r \rangle$ induces a tilt of the MnO_6 octahedra which results in the localization and ordering of $\text{Mn}^{3+}/\text{Mn}^{4+}$ cations. The disorder σ^2 and lattice distortion parameter (D) values are given in Table 1. Previously, the structural changes in Y doped CaMnO_3 have been reported by Vega et al. [15] from analysis of x-ray diffraction patterns at 300 K. They show the structure remains O- orthorhombic for $x \leq 0.25$, O+O' orthorhombic in the region $0.25 < x < 0.5$, and O' orthorhombic for $0.5 \leq x \leq 0.75$. Our results are in partial agreement with the previous studies where we find for $x \leq 0.1$ sample the structure remains O-type orthorhombic ($Pnma$ space group) in the whole temperature range while a transition from orthorhombic phase to monoclinic phase is observed in $x=0.2$ sample on lowering of temperature. Similar transition to monoclinic phase has been reported in some of the earlier studies on electron doped manganites [23–25]. The presence of the monoclinic phase has been correlated with the nature of magnetic ordering [6,7,23].

Table 1

Results of Rietveld refinement of neutron diffraction pattern at 6 K, resistivity values, Curie – Weiss fit parameters, and variance (σ^2) for $\text{Ca}_{1-x}\text{Y}_x\text{MnO}_3$.

	$x=0$ [27]	$x=0.1$	$x=0.2$	
			$Pnma$ (18%)	$P2_1/m$ (82%)
a (Å)	5.2771(10)	5.2895 (8)	5.3059 (3)	5.3456 (2)
b (Å)	7.4404(14)	7.4572(14)	7.4512 (14)	7.4225 (20)
c (Å)	5.2616(11)	5.2508(8)	5.2687 (9)	5.2821(2)
Volume (Å ³)	206.6	207.1	208.3	209.5
β (°)				91.1(3)
$\rho_{300\text{K}}$ (Ω-cm)	1.7 ± 0.4	1.4 ± 0.2	0.07 ± 0.01	
θ (K)	–510	–69	–96	
μ_{eff} (μ _B)	4.18	4.13	4.65	
$\sigma^2 \times 10^{-3}$		1	1.7	

Download English Version:

<https://daneshyari.com/en/article/1487456>

Download Persian Version:

<https://daneshyari.com/article/1487456>

[Daneshyari.com](https://daneshyari.com)